Atmos. Chem. Phys. Discuss., doi:10.5194/acp-2016-25, 2016
Manuscript under review for journal Atmos. Chem. Phys.
Published: 27 January 2016

Atmospheric Chemistry and Physics Discussions

Relation between ice and liquid water mass in mixed-phase cloud layers measured with Cloudnet

Johannes Bühl[1], Patric Seifert[1], Alexander Myagkov[1], and Albert Ansmann[1]
[1]Leibniz Institute for Tropospheric Research, Permoserstr. 15, 04318 Leipzig, Germany
Correspondence to: Johannes Bühl (buehl@tropos.de)

Abstract. An analysis of the Cloudnet dataset collected at Leipzig, Germany, with special focus on mixed-phase layered clouds is presented. We derive liquid and ice water content together with vertical motions of ice particles falling through cloud base. The ice mass flux is calculated by combining measurements of ice water content and particle fall velocity. The efficiency of heterogeneous ice formation and its impact on cloud lifetime is estimated for different cloud-top temperatures by relating the ice mass flux and the liquid water content at cloud top. Cloud radar measurements of polarization and fall velocity yield, that ice crystals formed in cloud layers with a geometrical thickness of less than 350 m are mostly pristine when they fall out of the cloud. It is also found that current and future spaceborne cloud radars might miss a large portion of that primary ice formation, especially for cloud layers with top temperatures warmer than $-15\,^{\circ}$C.

1 Introduction

Understanding the process of heterogeneous ice formation is currently one of the major topics in weather and climate research (Cantrell and Heymsfield, 2005; Hoose et al., 2008). Heterogeneous ice formation drives the generation of rain (Mülmenstädt et al., 2015), impacts cloud stability (Morrison et al., 2005) and atmospheric radiative transfer (Sun and Shine, 1994). It is therefore a crucial component in the hydrological cycle in the Earth's atmosphere. The interaction between aerosol and clouds in general involves very complex processes. Vertical motions keep mixed-phase clouds alive by activating aerosol particles to cloud droplets, while at the same time ice crystals nucleate and remove water from the cloud. To understand these complex interactions it is necessary to know all influences, process aspects and involved aerosol particles, cloud droplets, ice crystal ensembles as well as the spectrum of vertical air motions in detail. Laboratory measurements have already delivered a lot of useful information (Murray et al., 2012), observations of the process of ice nucleation in nature, however, are limited. By means of active remote sensing, however, quantities that are directly connected with ice nucleation events, e.g., the flux of ice crystals from cloud layers, can be measured. In the European Union research project BACCHUS (Impact of Biogenic versus Anthropogenic emissions on Clouds and Climate: towards a Holistic UnderStanding) the ice nucleating

Atmos. Chem. Phys. Discuss., doi:10.5194/acp-2016-25, 2016
Manuscript under review for journal Atmos. Chem. Phys.
Published: 27 January 2016

Atmospheric Chemistry and Physics Discussions
Open Access

properties of aerosols are investigated. It is one major task of this project to study the life cycle of aerosols from its source through the clouds by means of aircraft, in-situ and remote sensing observations. Combined remote sensing observations in the framework of Cloudnet (Illingworth et al., 2007) constitute one main pillar of the BACCHUS project.

Since 2011, the Leipzig Aerosol and Cloud Remote Observations System (LACROS) (Wandinger, 2012) belongs to the Cloudnet consortium. In this article, remote measurements of LACROS analyzed with Cloudnet algorithms are used to describe ice formation processes under ambient conditions. Such remote sensing measurements fill a critical gap in the study of mixed-phase processes, because they deliver the information about the entire cloud column from the base to the top, which is not possible with aircraft measurements alone. In this way, the temperature level at which ice nucleation takes place can be derived and at the same time the resulting ice water falling from the layer can be analyzed.

The focus of the present work is twofold: Firstly, quantitative statistics about ice and water mass in shallow mixed-phase cloud layers are derived from the Cloudnet dataset, taking into account values of each Cloudnet profile individually. This constitutes a step forward compared to Bühl et al. (2013) where properties of ice and cloud water have been analyzed separately and independently. Secondly, statistics about fall velocity and radar depolarization of the ice crystals are compiled in order to directly assess ice crystal sedimentation rates and to derive basic information about the shape of particles at the same time. (Not only quantitative knowledge about the particles themselves is gathered, but also the usability of cloud layers as atmospheric "laboratories" is characterized.) Only if ice crystals are pristine when falling from the cloud layer, there is a direct link between the properties of the ice (e.g., size, shape and mass) and their formation process within the cloud top layer. These measurements of ice particle properties are compared with laboratory studies of Fukuta and Takahashi (1999) in order to assess the quality of the Cloudnet measurements. Based on our dataset, the ice water content (IWC) produced by particles falling from cloud layers is derived and compared with the available liquid water within the cloud top layer. Together with the quality-assured fall velocity measurements a direct connection between the liquid water in the cloud top layer and the resulting ice mass flux is established, which can be regarded as a quantitative measure of heterogeneous ice formation in the atmosphere. With this approach, also the impact of ice formation on cloud lifetime is estimated for the temperature regime between -35 and $0\,^{\circ}$C.

All of the statistical analysis of ice formation in former studies (Kanitz et al., 2011; Bühl et al., 2013; Schmidt et al., 2015; Seifert et al., 2015), have been done manually. Such an approach is extremely time consuming and cloud selection criteria can not be applied on a fully objective basis. Until now, some Cloudnet stations have been running continuously for more than 10 years (e.g., Chilbolton and Lindenberg), providing each day a wealth of measurement values. Therefore, the analysis of clouds within such dataset can only be effective with an automated algorithm. For the present work, a method has been developed to automatically evaluate measurements from the Cloud-

Atmos. Chem. Phys. Discuss., doi:10.5194/acp-2016-25, 2016
Manuscript under review for journal Atmos. Chem. Phys.
Published: 27 January 2016

net dataset collected between 2011 and 2015 at TROPOS. A modified cloud-classification scheme from Bühl et al. (2013) is used to automatically discriminate liquid and mixed-phase cloud layers. The method is generally applicable to any Cloudnet dataset of arbitrary size. Hence, the method can be used to quickly analyze any dataset with the same objective criteria, and thus harmonizing Cloudnet measurements from all over the world.

Shallow mixed-phase cloud layers like altocumulus (Ac), altostratus (As) or stratocumulus (Sc) have been used before as atmospheric laboratories in order to study aerosol-cloud-dynamics interaction under ambient conditions. These cloud types are especially well suited for process studies purposes, because they show narrow constraints on basic environmental variables like temperature, pressure, humidity and the number of potentially involved microphysical processes (Tao and Moncrieff, 2009). The well defined base and top of shallow cloud layers is optimum to study aerosol effects on ice nucleation as well as the impact of up- and downdraft on cloud ice production. As an additional benefit, these shallow cloud layers can easily be penetrated by lidar and cloud radar systems, which is not possible for deep convective clouds due to massive signal attenuation and strong turbulence within their cores. For climate research these shallow cloud layers are important due to their hard-to-predict impact on Earth's radiative budget. From the meteorological point of view, the understanding of ice formation processes in deep convective mixed-phase clouds may be more important. However, such clouds and may not allow to resolve the basic ice processes and aerosol- and dynamics related aspects of ice formation. Both questions can be answered only by studying the process of ice formation itself in the atmosphere.

The paper is structured as follows. Section 2 gives a short overview about the dataset used in the context of this work. In Section 3 the methodology to analyze the dataset is presented. At the beginning of Section 4 the ice-detection capability of different cloud radar systems is analyzed. After that, quantitative statistics of ice and liquid water within mixed-phase cloud layers are derived.

2 Dataset

The data analyzed within the frame of this work has been collected with LACROS (Wandinger, 2012) at TROPOS Leipzig, Germany ($51.3°$ N, $12.4°$E) between 2011 and 2015. The time coverage of Cloudnet observations at Leipzig is about 85%. Instruments relevant for the present work are the PollyXT Raman/depolarization lidar (Althausen et al., 2009; Engelmann et al., 2015), the Jenoptik ceilometer CHM15kx, the MIRA-35 cloud radar (Görsdorf et al., 2015) and the HATPRO microwave radiometer. The measurements of these instruments are analyzed by the Cloudnet algorithms (Illingworth et al., 2007) to derive microphysical properties of hydrometeors on a continuous basis. Additionally model input of environmental variables like temperature and humidity is used. For the Cloudnet dataset of Leipzig, forecast data of COSMO-EU was used from 2011 to May 2014. Since June 2014, forecast data of the integrated forecast system of the European Centre for Medium-

Atmos. Chem. Phys. Discuss., doi:10.5194/acp-2016-25, 2016
Manuscript under review for journal Atmos. Chem. Phys.
Published: 27 January 2016

Range Weather Forecasts was used. In the rare cases, when this data is not available, COSMO-EU is used as a fall-back option. The resulting Cloudnet dataset is the basis for the following analysis of cloud layers over Leipzig presented in the following.

3 Automated selection and classification of cloud layers in a Cloudnet dataset

The automated Cloudnet algorithm reduces data from a set of remote sensing instruments on a common grid that has a temporal resolution of 30 s and a height resolution of 30.2 m (similar to the one of the cloud radar). In a further step, the physical state of the atmosphere in all height bins is classified into different categories, e.g., containing cloud droplets, ice particles or both. Other definitions concerning aerosol are also present, but do not play a role in the context of this work. A detailed description of the target categorization scheme of Cloudnet is given in Illingworth et al. (2007). Basically, liquid water droplets are detected by a threshold in lidar signal followed by a characteristic decrease of the latter above liquid cloud base. Ice particles are in general defined to be present if the radar-observed vertical velocity of the targets indicates falling particles and the dew-point temperature within a range gate is below 0 °C. If, in addition, the analysis of the lidar signal of the considered pixel meets the criteria for the presence of liquid droplets, the pixel is categorized as mixed-phase. The height of the melting layer is derived either from the meteorological data (dew-point temperature is 0 °C) or from an LDR measurement above −15 dB. Thus, the decision between liquid-only, mixed-phase or ice-only cloud layers is made primarily based on the modeled temperature and changes in the vertical-velocity profile. However, there is no way to unambiguously decide between drizzle and/or falling ice crystals.

For this work, an automated algorithm has been developed that runs on this basic target-classification product of Cloudnet. Single 30-s profiles are analyzed to search for liquid water. If liquid water is found, the base and top height of the liquid layer is stored and the height-range below this liquid water bin is searched for ice. If ice is found below, also the height of transition between liquid and ice is stored. This procedure is done for all profiles of the dataset. Afterwards neighboring cloud profiles are merged if they lie within 300 s of temporal and 350 m of vertical distance. A set of connected profiles constitutes a cloud for which we assume that the driving microphysics are similar throughout the whole cloud layer. For the statistical analysis, a cloud must pass certain quality criteria: A coherent cloud structure must be found for more than 20 minutes, no seeding of particles from higher-level clouds must be present and at least 85% of the cloud's occurrence time a liquid or mixed-phase cloud top must be detected. The properties of the detected clouds, e.g., cloud-top height (CTH), geometrical cloud thickness δ_h, standard-deviation of cloud-top height σ_{CTH}, cloud-top temperature (CTT), radar reflectivity factor (Z), ice-water content (IWC), liquid-water content (LWC), LDR, lidar attenuated backscatter coefficient (β) and lidar volume linear depolarization ratio are stored for further analysis. See Fig. 1 for an overview where the different properties are derived

Atmos. Chem. Phys. Discuss., doi:10.5194/acp-2016-25, 2016
Manuscript under review for journal Atmos. Chem. Phys.
Published: 27 January 2016

Atmospheric Chemistry and Physics Discussions

for one cloud case. The picture also shows, that some measurement values are taken only from a height-level 60 m below the mixed-phase cloud base. At this point, cloud droplets should be absent and ice particles should still be largely unaltered by evaporation or aggregation processes. Hence their size and shape should only be related to processes having taken place within the mixed-phase cloud top layer. In the context of this work, all measurement values derived in this way are marked with the index "CB" (for "cloud base").

After cloud identification, the cloud-classification scheme from Bühl et al. (2013) is used to discriminate between liquid and mixed-phase cloud layers (see Fig. 2). This classification method reduces the dependence on model temperature by taking into account information from all cloud profiles to make a decision between the microphysical states "liquid" or "mixed-phase". Depolarization measurements from lidar and radar are used to directly identify ice crystals falling from a cloud layer. Mixed-phase clouds close to $0\,^{\circ}$C also often show a melting layer, which is the most unambiguous sign of the presence of ice particles (Di Girolamo et al., 2012). High LDR values are also produced by the needle-like ice crystals prevailing for clouds with a CTT between -8 and $-2\,^{\circ}$C (Fukuta and Takahashi, 1999). Such clear LDR signal make the decision between ice and liquid water fortunately very easy close to the $0\,^{\circ}$C level, where model temperature in most cases is not accurate enough and the increase in particle fall speed due to melting is not significant. For low signal-to-noise ratios (SNR) of $-10...0$ dB and no detection of a melting layer, the depolarized signal is usually too weak to be detected by the cross-polarized channel of the MIRA-35 cloud radar. In this case, measurements of volume linear depolarization ratio from a collocated PollyXT lidar is used (Engelmann et al., 2015), if available. In Fig. 3 three example cases with different CTT from different dates are shown together. Cloud radar measurements of Z, LDR and v are shown together with the attenuated backscatter coefficient from the lidar. The CTT of the three cases are chosen in such a way that distinct differences in LDR measurements are visible between the cases. As an example for cloud detection/selection, all clouds with $\delta_h < 350$ m and $\sigma_{\mathrm{CTH}} < 150$ m detected on 2 October 2012 at Leipzig are marked in Fig. 4. The CTT statistics of all selected and classified cloud layers with these selection criteria ($\delta_h < 350$ m and $\sigma_{\mathrm{CTH}} < 150$ m) are shown in Figs. 5a and 5b. It is visible that no mixed-phase clouds are detected below $-40\,^{\circ}$C.

4 Quantitative description of heterogeneous ice formation in cloud layers over Leipzig

4.1 Ice-mass retrieval and detection thresholds

A quantitative retrieval of ice mass is done by Cloudnet via the method of Hogan et al. (2006). IWC values are obtained for each range bin with a simple empirical function depending on Z and the ambient temperature. The uncertainty of the method is estimated by Hogan et al. (2006) to be $(+50/-30)\%$ below a temperature of $-10\,^{\circ}$C and $(+100/-50)\%$ above. Uncertainties in the measurements of Z add to these errors. Hence, for the quantitative understanding of ice formation in the

Atmos. Chem. Phys. Discuss., doi:10.5194/acp-2016-25, 2016
Manuscript under review for journal Atmos. Chem. Phys.
Published: 27 January 2016

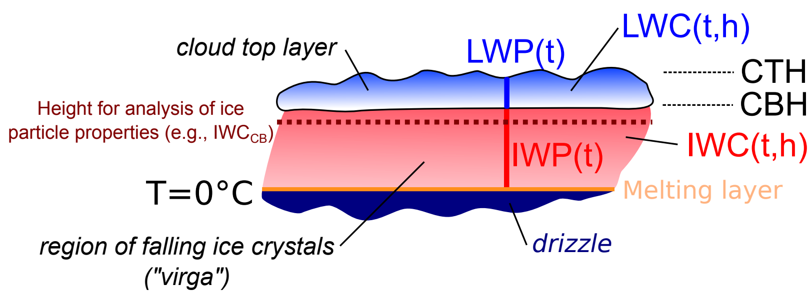

Figure 1. Schematic representation of the different measurement and averaging schemes in a mixed-phase cloud layer. On top the predominantly liquid water top is detected by lidar. The ice precipitation below is mainly detected by the cloud radar. IWC and LWC are provided by Cloudnet and are a function of height (h) and time (t). IWP and LWP are the column integrated values of LWC and IWC over the liquid cloud top and the ice precipitation, respectively. IWC_{CB} represents the mean of all IWC values measured about 60 m below current cloud base height (CBH).

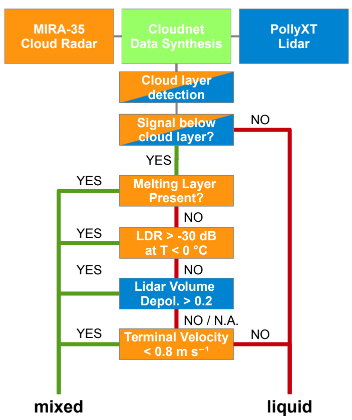

Figure 2. Flowchart of the mixed-phase cloud discrimination method from Bühl et al. (2013) as it is applied in the current work. Most clouds are successfully analyzed with combined lidar/radar.

Atmos. Chem. Phys. Discuss., doi:10.5194/acp-2016-25, 2016
Manuscript under review for journal Atmos. Chem. Phys.
Published: 27 January 2016

Atmospheric Chemistry and Physics
Open Access
Discussions

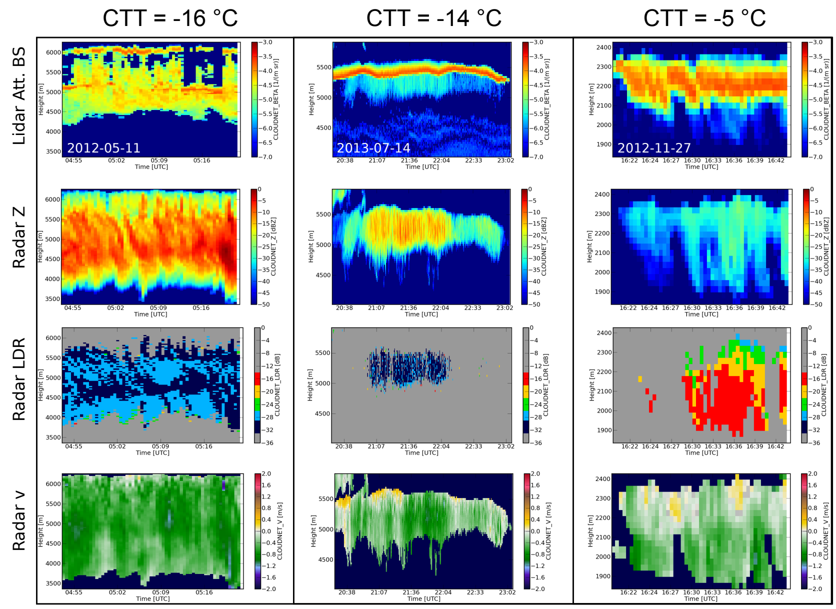

Figure 3. Three example case-studies of mixed-phase clouds identified with the automated algorithm described in Section 3.

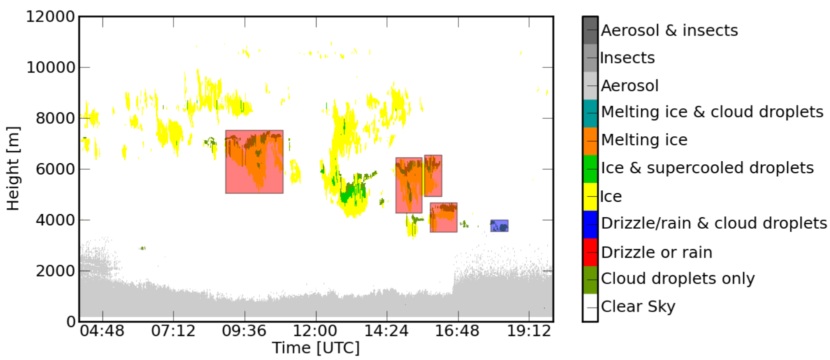

Figure 4. Example of automated detection of mixed-phase cloud layers on the basis of the Cloudnet target classification scheme for 2 October 2012. Blue squares mark liquid-only layers and red squares mark mixed-phase layers. The colors are only for a very basic visualization of the layer detection. The decision between mixed-phase and liquid clouds in the following analysis is more complex and described in the text.

Atmos. Chem. Phys. Discuss., doi:10.5194/acp-2016-25, 2016
Manuscript under review for journal Atmos. Chem. Phys.
Published: 27 January 2016

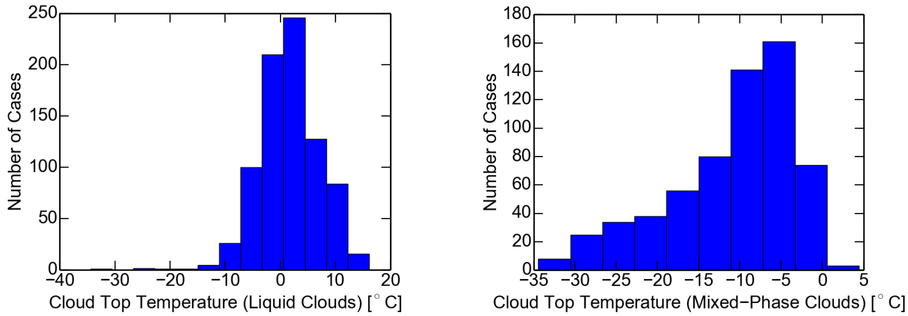

(a) (b)

Figure 5. Distribution of cloud-top temperature for all pure liquid (a) and mixed phase (b) cloud layers detected between 2011 and 2015 over Leipzig.

atmosphere, knowledge about the accuracy and – especially – about the signal detection threshold of the cloud radar is critical. In the case of ground-based radar, different factors can affect the measured values of Z, e.g., unknown attenuation in rain and uncertainties in radar calibration. Strong attenuation is avoided by excluding clouds from the analysis that are measured above other clouds or rain. Radar calibration is estimated to be accurate to $3\,$dB for the LACROS cloud radar, resulting in an additional bias in the IWC retrieval of about 30%, making them an estimation within the order of magnitude.

The starting point for the characterization of the IWC dataset is Fig. 6. In this figure, the signal-to-noise ratio (SNR) detected within cloud virgae (streams of ice particles falling from cloud top) is depicted together with the detected average LDR (color scale). The LACROS cloud radar can detect a signal down to an SNR of $-23\,$dB. From Fig. 6 it becomes obvious that particle detection at higher temperatures above $-10\,°$C are often close to the detection limit. In this temperature regime, the detection of some ice below cloud bases might be missed and clouds could be erroneously be classified as liquid-clouds. In contrast, ice detection seems to be quite reliable below $-10\,°$C, where all cases have a mean SNR well above the detection threshold. It is also visible from the figure, that LDR values can only be detected if a certain SNR threshold is reached.

Figure 7a depicts all measurements of Z_{CB} sorted by CTT. In Fig. 7b the values of Z_{CB} are shown averaged for individual cloud cases. The equivalent values of $\mathrm{IWC}_{\mathrm{CB}}$ are shown in Fig. 7c. Detection thresholds of $Z_{\mathrm{thr}} = 5000.0/r^2 \times (-45)\,$dBZ and $\mathrm{IWC}_{\mathrm{thr}}$ for different radar systems are drawn within the plots. Please note that the ice detection threshold is not only depending on the radar signal threshold, but also on temperature. For spaceborne systems Z_{thr} is nearly constant for the complete troposphere. The measurement distance of about $400-800\,$km leads to a range-induced signal variation of maximum 5% between 0 and $12\,$km height. For ground-based systems, however, the detection threshold varies dramatically for different heights. This phenomenon is depicted in Fig. 7d, where

Atmos. Chem. Phys. Discuss., doi:10.5194/acp-2016-25, 2016
Manuscript under review for journal Atmos. Chem. Phys.
Published: 27 January 2016

Atmospheric Chemistry and Physics
Open Access
Discussions

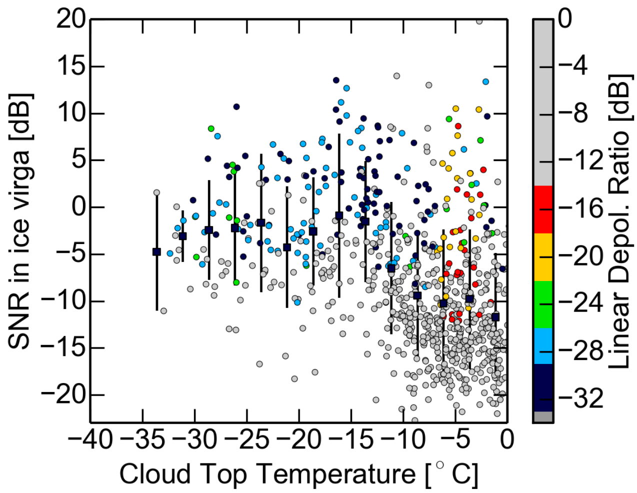

Figure 6. The 90% percentile of cloud-radar SNR is shown for each cloud case together with mean detected LDR.

mean Z_{CB} is plotted against CTH instead of CTT. The height-dependent detection threshold of the LACROS cloud radar is shown in red.

4.2 Sensitivity of measurements on geometrical cloud thickness

Fukuta and Takahashi (1999) provide comprehensive laboratory measurements of the growth of ice crystals. They found different distinct features in the resulting shape of ice crystals for different growth times and calculated corresponding residence times within a cloud layer, taking into account increasing fall speed with increasing particle size. For a residence time of 20 minutes within a mixed-phase cloud layer, particles could still be considered pristine. Also Yano and Phillips (2010) found that within this time, secondary processes like riming do not influence heterogeneous ice formation significantly. According to Fukuta and Takahashi (1999), a residence time of 20 minutes corresponds to a geometrical thickness of a mixed-phase cloud top layer of 350 m. Hence, for the present study only clouds with a geometrical thickness of below 350 m were selected to avoid altering of the ice crystals by riming, splintering or aggregation processes.

The necessity to select thin clouds in order to analyze pristine ice crystals is demonstrated in Fig. 8, where, in contrast to Fig. 7c, cloud layers up to a geometrical thickness of 600 m are taken into account. For this cloud height, the residence time of the ice crystals within the mixed-phase cloud layer is about 30 min. Accordingly, the detected ice mass becomes considerably larger, especially in the temperature range between -8 and $0\,^{\circ}$C where the efficiency of ice multiplication processes (Hallett and Mossop, 1974) is known to be largest. On the other hand, it is visible from Fig. 8 that

Atmos. Chem. Phys. Discuss., doi:10.5194/acp-2016-25, 2016
Manuscript under review for journal Atmos. Chem. Phys.
Published: 27 January 2016

Atmospheric Chemistry and Physics
Open Access
Discussions

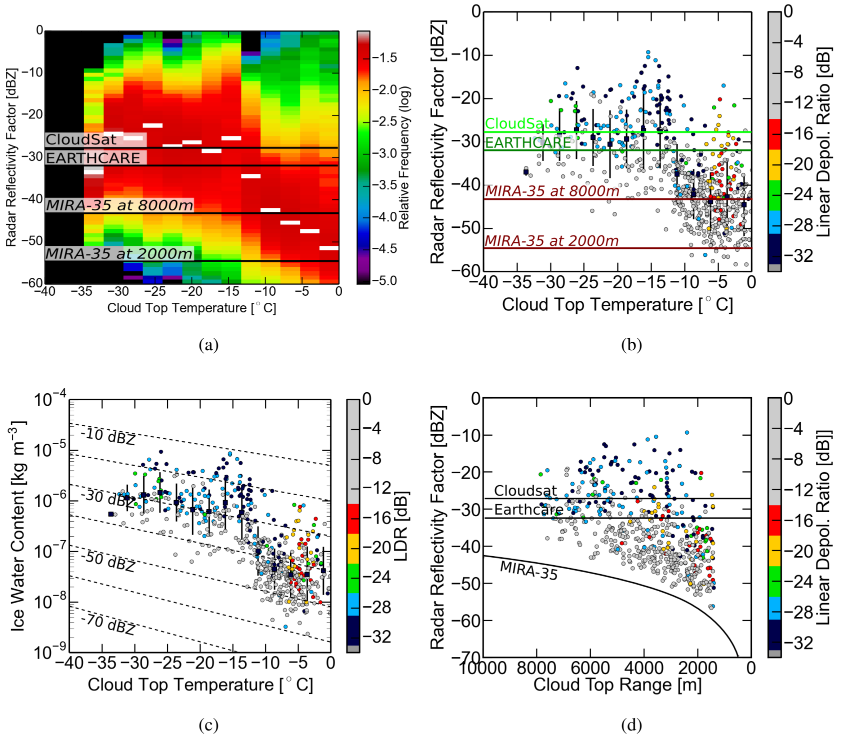

Figure 7. (a) All values of Z_{CB} column-normalized, (b) Z_{CB} averaged for each cloud case together with averaged LDR values, (c) $\mathrm{IWC_{CB}}$ averaged for each cloud case, (d) values of Z_{CB} depicted depending on CTH instead of CTT. Thresholds for Z and IWC are illustrated within the graphs.

the relaxation of selection criteria can increase the number of cases. Consequently, the statistics of LDR becomes more significant and some effects are better visible. At temperatures below $-22\,°\mathrm{C}$, e.g., it can be seen that low values of LDR accumulate for the highest ice mass concentrations of $10^{-5}\,\mathrm{kg\,m^{-3}}$, which gives a hint towards the presence of aggregation processes in these cases. The analysis within this paper is restricted to a cloud thickness of less than 350 m, in order to derive ice properties that are only related to primary ice production.

4.3 Fall velocity and radar depolarization of pristine ice crystals

In contrast to the extensive properties Z_{CB} and $\mathrm{IWC_{CB}}$, the measurements of the cloud radar can also be used to derive the intensive properties of the ice crystals (e.g., v and LDR). The latter are connected to size, shape and orientation of the ice particles. Values of LDR and v_{CB} averaged for each cloud case are shown in Figs. 9c and 9d. One has to keep in mind that LDR is dependent both on particle shape and particle orientation, so this information is not unambiguous (Reinking et al.,

Atmos. Chem. Phys. Discuss., doi:10.5194/acp-2016-25, 2016
Manuscript under review for journal Atmos. Chem. Phys.
Published: 27 January 2016

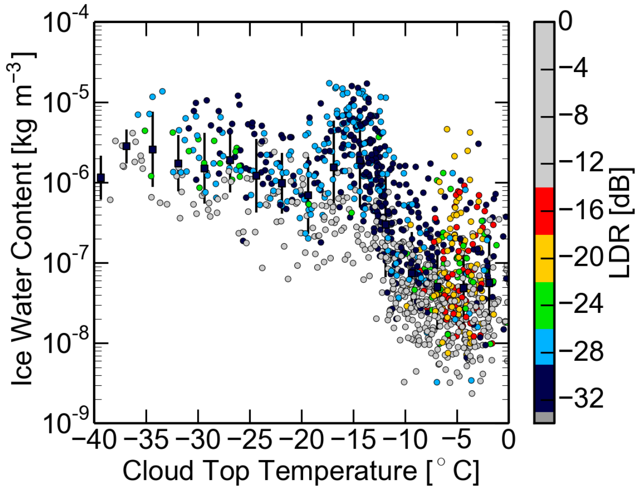

Figure 8. IWC_{CB} for an extended dataset with cloud layers included that are up to 600 m thick (instead of 350 m in Fig. 7c).

1997). However, if particles are oriented, which is the case if particles fall in a certain regime of the Reynolds number (Mitchell, 1996), high LDR values indicate prolate (column-shaped) particles and low values point towards more oblate particles like dendrites. For randomly oriented aspherical particles, LDR is always elevated. In this way, LDR gives only basic information about particle shape, but LDR has the advantage that it can be derived easily together with v_{CB} values with a vertical pointing radar.

The raw values of LDR and v_{CB} from all cases are shown in Figs. 9a and 9b. The values are taken from the virgae where the target classification of Cloudnet states “ice only”. These representations already show interesting features. In Fig. 7a, e.g., it has already been shown that at temperatures above $-10\,°C$ the average value of Z_{CB} is often below -30 dBZ. The depolarization measurements show a clear feature of elevated LDR values in this temperature range, pointing towards the presence of highly prolate and oriented ice particles. The vertical velocity measurements in 9b also show features of enhanced fall velocities indicating the different prevailing particle habits over the temperature range of heterogeneous ice formation.

Fukuta and Takahashi (1999) also found several distinct features in the distribution of ice particle size, shape and mass with temperature. Some of these features can be seen within the measurements of LDR and v_{CB}:

– An enhanced growth of ice crystal mass around $-14\,°C$ was found by Fukuta and Takahashi (1999). The effect can also be seen in Figs. 7a and Fig. 7b as a strong increase of Z_{CB} at this

Atmos. Chem. Phys. Discuss., doi:10.5194/acp-2016-25, 2016
Manuscript under review for journal Atmos. Chem. Phys.
Published: 27 January 2016

Atmospheric Chemistry and Physics Discussions
Open Access
EGU

temperature. The cloud radar is sensitive to the square of the particle mass and reacts therefore very sensitive on changes of this quantity.

– The high values of LDR measured at a CTT of $-5\,°C$ correspond to a needle- or column-like particle shape (see Figs. 9a and 9c). In the temperature range around $-14\,°C$ LDR values can be found to be around $-28\,dB$, corresponding to plate-like crystal shapes. Please note that these features are also displayed in Fig. 3. In Reinking et al. (1997) the LDR values values of -15 to $-20\,dB$ are computed for these ice crystals shapes.

– Hints on the presence of these isometric ice crystals are found in the increase of fall velocity in Fig. 9d. Measured fall velocities peak at around -10 and $-22\,°C$, while minima of LDR can be found at -12 and $-22\,°C$. This connection also points towards more isometric ice crystals around these temperatures.

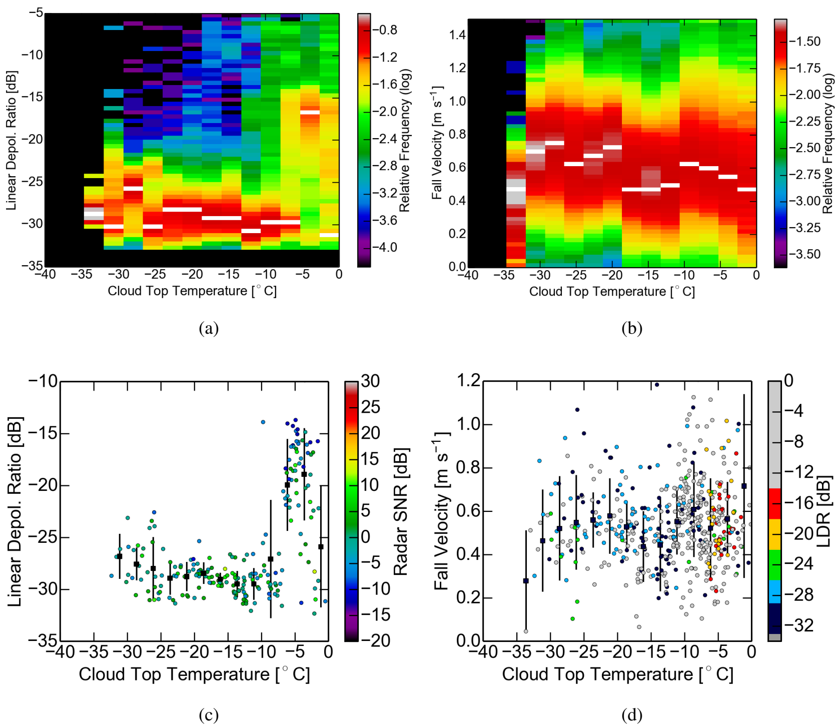

Figure 9. All values of (a) LDR and (b) v_{CB} measured with cloud radar MIRA-35 in the virgae below cloud layers over Leipzig. Averaged values for the indivdual cloud cases are depicted in (c) and (d), respectively. Maximum values in each column are marked with white bars.

Atmos. Chem. Phys. Discuss., doi:10.5194/acp-2016-25, 2016
Manuscript under review for journal Atmos. Chem. Phys.
Published: 27 January 2016

4.4 Relation between IWC_{CB} and LWC at cloud top

In the previous sections the properties of the ice particles produced within mixed-phase clouds was investigated. For the estimation of cloud stability by static approaches like the one presented by Korolev and Field (2008), however, the ice- to liquid water content ratio (ILCR) is important. Given a known flux of ice mass from a liquid cloud layer, the ILCR determines the lifetime of the cloud layer. In the following, approaches are presented to derive ILCR, ice mass flux and cloud life time from the mixed-phase cloud dataset presented above.

The liquid-water content (LWC) of a cloud layer is calculated for each cloud profile adiabatically between cloud bases and cloud tops. Cloudnet also provides operationally adiabatic profiles scaled with the LWP measured with the microwave radiometer (Pospichal et al., 2012). However, the LWP measurements of the microwave radiometer have an uncertainty of about $\pm 20\,\mathrm{g\,m^2}$. Since the average liquid water path of the cloud under study is actually around $20\,\mathrm{g\,m^2}$, the adiabatically calculated profiles are probably more accurate than those measured by the microwave radiometer and therefore preferred in the context of this work. An overview about the LWP of all cloud layers under study is given in Fig. 10a.

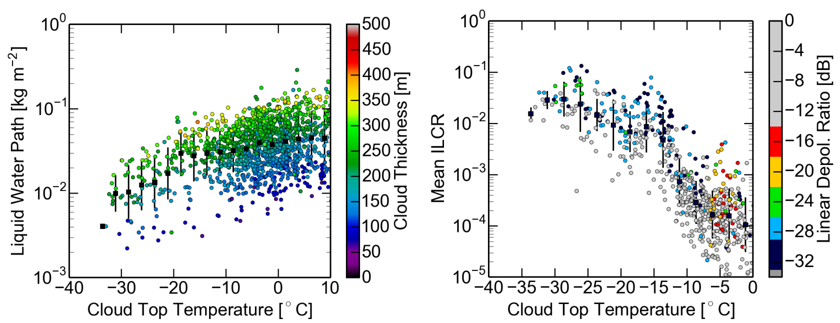

(a) (b)

Figure 10. (a) LWP of all clouds under study is shown in dependence of temperature and mean cloud top thickness. (b) The ratio between IWC_{CB} and mean LWC is calculated for each cloud-profile and average for each cloud case.

In Fig. 10b, IWC_{CB} is divided by the mean LWC at cloud top to derive an estimate of ILCR.

4.5 Estimating the ice mass flux from a cloud layer

The ILCR connects measurements of ice and liquid water mass. However, ice formation is a dynamic process: Ice crystals created inside the cloud top layer are falling with a terminal velocity $v_{CB} > 0.2\,\mathrm{m\,s^{-1}}$ (see Fig. 9d, while the majority of cloud droplets have negligible fall velocity. The same number of particles creates a different IWC when falling at different terminal velocities, because the

Atmos. Chem. Phys. Discuss., doi:10.5194/acp-2016-25, 2016
Manuscript under review for journal Atmos. Chem. Phys.
Published: 27 January 2016

stream of particles is actually "stretched" differently. Hence, the ice flux $F = \mathrm{IWC_{CB}} \times v$ at cloud base gives the most accurate description of ice formation per time interval inside the cloud top layer. In this very simple picture, F describes the flux rather coarsely. Since IWC and v are both closely related to the strongest peak of the cloud radar spectrum, direct multiplication actually makes sense. The resulting parameter may however be an estimation within the order of magnitude and may only have a meaning relative to other flux values, calculated in the same way. Figure 11a displays averaged F for all cloud cases under study. Especially at temperatures below $-20\,^\circ\mathrm{C}$ it can be seen that the flux of ice mass is only weakly depending on temperature. In this temperature range $\mathrm{IWC_{CB}}$ (Fig. 7c) is decreasing with temperature while v (Fig. 9d) is increasing. Also the peak at $-15\,^\circ\mathrm{C}$ is less pronounced compared to Figs. 7b and 7c as it coincides with a minimum in particle fall velocity.

The concept of ice mass flux also opens the possibility to derive basic information about the impact of ice formation on cloud lifetime. Water particles most probably glaciate at cloud top and fall through the mixed-phase layer. Having connected v with with $\mathrm{IWC_{CB}}$ to the ice flux, it is also possible to relate this quantity to the available LWP within the ice-generating liquid cloud layer. Since ice particles grow through the Wegener-Bergeron-Findeisen process (Korolev and Field, 2008), there is an indirect connection between the amount of available water vapor and ice crystal growth. Hence, a dynamic view of ice formation in the cloud layers can be established by dividing F and LWP profile-wise.

$$\frac{LWP}{F} = \frac{LWP}{\mathrm{IWC_{CB}} \times v} \stackrel{!}{=} T_l, \qquad (1)$$

Defined in this way, T_l is a time measured in seconds. Assuming steady conditions T_l is the time the liquid cloud top layer would have depleted all its liquid water by ice sedimentation alone. It is a theoretical quantity, but it gives an impression of the relative impact of ice on different cloud layers. Figure 11b shows that T_l is typically larger than one day for all observed cloud cases.

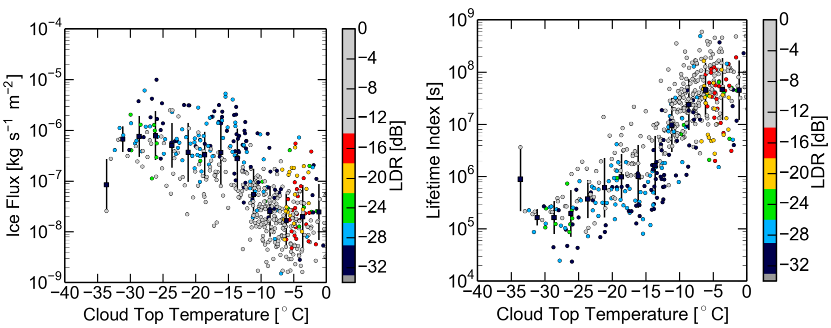

(a)　　(b)

Figure 11. (a) The ice mass flux at cloud base. (b) The estimated lifetime index $t_l = \mathrm{LWP}/F$ of each cloud.

Atmos. Chem. Phys. Discuss., doi:10.5194/acp-2016-25, 2016
Manuscript under review for journal Atmos. Chem. Phys.
Published: 27 January 2016

Atmospheric Chemistry and Physics Discussions

5 Summary and Conclusions

Quantitative retrievals of ice crystal properties like basic information about particle shape and fall velocity have been found to be quantitatively in line with theoretical computations of Reinking et al. (1997) and laboratory studies of Fukuta and Takahashi (1999). Ice particles falling from mixed-phase cloud layers with a geometrical thickness of the mixed-phase top layer < 350 m seem to be mostly pristine. Additionally, a profile-based connection between the measured liquid water path (LWP) and the retrieved IWC has been established. It has been shown that the ice-mass formed within a mixed-phase cloud layer can be estimated within one order of magnitude from LWP and CTT. The flux of ice mass at cloud base height is found to increase within two orders of magnitude within the CTT range from -40 to $0\,°$C. The relative influence of the loss of ice on cloud lifetime is found to increase even by 4 orders of magnitude within the same range of CTT.

It is demonstrated in this work that a detailed insight into the microphysics of mixed-phase cloud layers is possible with LACROS and Cloudnet. Vertical velocity measurements show the dynamical state of the turbulent layer and cloud radar measurements show the ice flux from that layer. Together with the retrieval of ice nuclei properties with Raman lidar (Mamouri and Ansmann, 2015) the life cycle of an ice nucleus in mixed-phase clouds from entrainment over activation to ice nucleation and sedimentation can be closed.

It is also an important finding that shallow mixed-phase cloud layers with $\delta_h < 350$ m mainly produce pristine ice. This means that the flux of ice crystals measured at cloud base is directly connected to the rate of ice nucleation within the mixed-phase layer. The direct measurement of the complete process of ice nucleation seems therefore feasible with remote sensing. However, in future, more advanced particle typing methods such as presented in Myagkov et al. (2015a, b) should be applied to further characterize shape and size of the particles on an operational basis.

The relative impact of the loss of ice water on a mixed-phase cloud layer can be measured. However, it has to be noted again, that the cloud lifetime parameter presented here might not directly be connected to the absolute lifetime of a cloud. Even the definition of a cloud lifetime is difficult, because particles are mixed between cloud parcels and the apparent motion of clouds can be independent from horizontal wind speed. However, the cloud lifetime parameter presented here can be used to study the impact of ice on predominantly liquid cloud layers occurring at different temperature levels. Measurements of ice mass flux and the cloud lifetime parameter T_l indicate a minimum cloud layer lifetime of 3 hours around $-25\,°$C. At temperatures above $-15\,°$C the relative impact of ice formation has already shrunk by 2 orders of magnitude. Given the fact that Korolev and Field (2008) showed that the cloud layers under study here actually are able to recreate liquid water via recurring upward air motion, these clouds seem to be extremely stable with respect to water depletion due to ice formation. The lifetime parameter is a considerable step forward compared to Bühl et al. (2013), where the mass ratio of ice and liquid water in mixed-phase layered clouds was estimated with a ratio of IWP and LWP on manually selected clouds. The ratio of $\mathrm{IWC_{CB}}$ and LWP, combined with the particle fall velocity gives a much more direct measure of the actual impact of the ice on the liquid water within a mixed-phase layer.

The presented algorithm to classify mixed-phase clouds in Cloudnet datasets is universal. It is not only applicable on Cloudnet datasets, but in general on all datasets that separate an atmospheric column into liquid, ice and mixed-phase. The evaluation of mixed-phase clouds predicted by weather models seems therefore possible if suitable data output is given. The established relation between LWP and $\mathrm{IWC}_{\mathrm{CB}}$ could also be used as a parameterization to derive the mass of ice from the LWP alone in numerical models.

The LACROS cloud radar has a depolarization decoupling of -33 dB, which stands out from all radars currently operated within the framework of Cloudnet. Only this technical prerequisite makes high-quality measurements of LDR possible. Also the detection threshold of -47 dBZ at a range of 5000 m is outstanding. Satellite missions equipped with cloud radars like Cloudsat (Stephens et al., 2002) and EarthCare (Illingworth et al., 2014) have detection thresholds within the troposphere of -27 dBZ and -33 dBZ respectively. Hence, these satellites will miss probably more than 90% of the ice-signals below mid-latitudinal cloud layers with a CTT above $-10\,^{\circ}$C (see Fig. 7a).

Acknowledgements. The research leading to these results has received funding from the European Union Seventh Framework Programme (FP7/2007-2013) under grant agreement numbers 262254 (ACTRIS) and 603445 (BACCHUS) and from the HD(CP)^2 project of the German Ministry for Education and Research.

References

Althausen, D., Engelmann, R., Baars, H., Heese, B., Ansmann, A., Müller, D., and Komppula, M.: Portable Raman lidar PollyXT for automated profiling of aerosol backscatter,extinction, and depolarization, Journal of Atmospheric and Oceanic Technology, 26, 2366–2378, http://dx.doi.org/10.1175/2009JTECHA1304.1, 2009.

Bühl, J., Ansmann, A., Seifert, P., Baars, H., and Engelmann, R.: Towards a quantitative characterization of heterogeneous ice formation with lidar/radar: Comparison of CALIPSO/CloudSat with ground-based observations, Geophysical Research Letters, 40, 4404–4408, doi:10.1002/grl.50792, http://dx.doi.org/10.1002/grl.50792, 2013.

Cantrell, W. and Heymsfield, A.: Production of Ice in Tropospheric Clouds: A Review, Bull. Amer. Meteor. Soc., 86, 795–807, doi:10.1175/BAMS-86-6-795, http://dx.doi.org/10.1175/BAMS-86-6-795, 2005.

Di Girolamo, P., Summa, D., Cacciani, M., Norton, E. G., Peters, G., and Dufournet, Y.: Lidar and radar measurements of the melting layer: observations of dark and bright band phenomena, Atmospheric Chemistry and Physics, 12, 4143–4157, doi:10.5194/acp-12-4143-2012, http://www.atmos-chem-phys.net/12/4143/2012/, 2012.

Engelmann, R., Kanitz, T., Baars, H., Heese, B., Althausen, D., Skupin, A., Wandinger, U., Komppula, M., Stachlewska, I. S., Amiridis, V., Marinou, E., Mattis, I., Linné, H., and Ansmann, A.: EARLINET Raman Lidar Polly^{XT}: the neXT generation, Atmospheric Measurement Techniques Discussions, 8, 7737–7780, doi:10.5194/amtd-8-7737-2015, http://www.atmos-meas-tech-discuss.net/8/7737/2015/, 2015.

Fukuta, N. and Takahashi, T.: The Growth of Atmospheric Ice Crystals: A Summary of Findings in Vertical Supercooled Cloud Tunnel Studies, J. Atmos. Sci., 56, 1963–1979, http://dx.doi.org/10.1175/1520-0469(1999)056<1963:TGOAIC>2.0.CO;2, 1999.

Görsdorf, U., Lehmann, V., Bauer-Pfundstein, M., Peters, G., Vavriv, D., Vinogradov, V., and Volkov, V.: A 35-GHz Polarimetric Doppler Radar for Long-Term Observations of Cloud Parameters—Description of System and Data Processing, J. Atmos. Oceanic Technol., 32, 675–690, http://dx.doi.org/10.1175/JTECH-D-14-00066.1, 2015.

Hallett, J., J. and Mossop, S. C.: Production of secondary ice particles during the riming process, Nature, 249, 26–28, http://dx.doi.org/10.1038/249026a0, 1974.

Hogan, R. J., Mittermaier, M. P., and Illingworth, A. J.: The retrieval of ice water content from radar reflectivity factor and temperature and its use in evaluating a mesoscale model, Journal of Applied Meteorology and Climatology, 45, 301–317, http://dx.doi.org/10.1175/JAM2340.1, 2006.

Hoose, C., Lohmann, U., Erdin, R., and Tegen, I.: The global influence of dust mineralogical composition on heterogeneous ice nucleation in mixed-phase clouds, Environmental Research Letters, 3, 025 003, http://stacks.iop.org/1748-9326/3/i=2/a=025003, 2008.

Illingworth, A. J., Hogan, R. J., O'Connor, E. J., Bouniol, D., Delanoë, J., Pelon, J., Protat, A., Brooks, M. E., Gaussiat, N., Wilson, D. R., Donovan, D. P., Baltink, H. K., van Zadelhoff, G.-J., Eastment, J. D., Goddard, J. W. F., Wrench, C. L., Haeffelin, M., Krasnov, O. A., Russchenberg, H. W. J., Piriou, J.-M., Vinit, F., Seifert, A., Tompkins, A. M., and Willén, U.: Cloudnet, Bulletin of the American Meteorological Society, 88, 883–898, http://dx.doi.org/10.1175/BAMS-88-6-883, 2007.

Illingworth, A. J., Barker, H. W., Beljaars, A., Ceccaldi, M., Chepfer, H., Cole, J., Delanoë, J., Domenech, C., Donovan, D. P., Fukuda, S., Hirakata, M., Hogan, R. J., Huenerbein, A., Kollias, P., Kubota, T., Nakajima, T., Nakajima, T. Y., Nishizawa, T., Ohno, Y., Okamoto, H., Oki, R., Sato, K., Satoh, M., Shephard, M., Wandinger, U., Wehr, T., and van Zadelhoff, G.-J.: THE EARTHCARE SATELLITE: The next step forward in global measurements of clouds, aerosols, precipitation and radiation., Bull. Amer. Meteor. Soc., pp. –, http://dx.doi.org/10.1175/BAMS-D-12-00227.1, 2014.

Kanitz, T., Seifert, P., Ansmann, A., Engelmann, R., Althausen, D., Casiccia, C., and Rohwer, E. G.: Contrasting the impact of aerosols at northern and southern midlatitudes on heterogeneous ice formation, Geophysical Research Letters, 38, L17802, doi:10.1029/2011GL048532, http://dx.doi.org/10.1029/2011GL048532, 2011.

Korolev, A. and Field, P. R.: The effect of dynamics on mixed-phase clouds: Theoretical considerations, Journal of Atmospheric Sciences, 65, 66–86, doi:10.1175/2007JAS2355.1, 2008.

Mamouri, R. E. and Ansmann, A.: Estimated desert-dust ice nuclei profiles from polarization lidar: methodology and case studies, Atmospheric Chemistry and Physics, 15, 3463–3477, doi:10.5194/acp-15-3463-2015, http://www.atmos-chem-phys.net/15/3463/2015/, 2015.

Mitchell, D. L.: Use of mass- and area-dimensional power laws for determining precipitation particle terminal velocities, Journal of the Atmospheric Sciences, 53, 1710–1723, http://dx.doi.org/10.1175/1520-0469(1996)053<1710:UOMAAD>2.0.CO;2, 1996.

Morrison, H., Shupe, M. D., Pinto, J. O., and Curry, J. A.: Possible roles of ice nucleation mode and ice nuclei depletion in the extended lifetime of Arctic mixed-phase clouds, Geophysical Research Letters, 32, L18801, doi:10.1029/2005GL023614, 2005.

Mülmenstädt, J., Sourdeval, O., Delanoë, J., and Quaas, J.: Frequency of occurrence of rain from liquid-, mixed-, and ice-phase clouds derived from A-Train satellite retrievals, Geophysical Research Letters, 42, 6502–6509, doi:10.1002/2015GL064604, 2015.

Murray, B., O'Sullivan, D., Atkinson, J., and Webb, M.: Ice nucleation by particles immersed in supercooled cloud droplets, Chemical Society reviews, 41, 6519–6554, 2012.

Myagkov, A., Seifert, P., Bauer-Pfundstein, M., and Wandinger, U.: Cloud radar with hybrid mode towards estimation of shape and orientation of ice crystals, Atmospheric Measurement Techniques Discussions, 8, 9105–9163, doi:10.5194/amtd-8-9105-2015, http://www.atmos-meas-tech-discuss.net/8/9105/2015/, 2015a.

Myagkov, A., Seifert, P., Wandinger, U., Bühl, J., and Engelmann, R.: Shape-temperature relationships of pristine ice crystals derived from polarimetric cloud radar observations during the ACCEPT campaign, Atmospheric Measurement Techniques Discussions, 0, 0–0, doi:0, 0, 2015b.

Pospichal, B., Kilian, P., and Seifert, P.: Performance of cloud liquid water retrievals from ground-based remote sensing observations over Leipzig, in: Proceedings of the 9th International Symposium on Tropospheric Profiling(ISTP), L'Aquila, 2012.

Reinking, R. F., Matrosov, S. Y., Bruintjes, R. T., and Martner, B. E.: Identification of hydrometeors with elliptical and linear polarization Ka-band radar, Journal of Applied Meteorology and Climatology, 36, 322–339, http://dx.doi.org/10.1175/1520-0450(1997)036<0322:IOHWEA>2.0.CO;2, 1997.

Schmidt, J., Ansmann, A., Bühl, J., and Wandinger, U.: Strong aerosol–cloud interaction in altocumulus during updraft periods: lidar observations over central Europe, Atmospheric Chemistry and Physics, 15, 10 687–10 700, doi:10.5194/acp-15-10687-2015, http://www.atmos-chem-phys.net/15/10687/2015/, 2015.

Seifert, P., Kunz, C., Baars, H., Ansmann, A., Bühl, J., Senf, F., Engelmann, R., Althausen, D., and Artaxo, P.: Seasonal variability of heterogeneous ice formation in stratiform clouds over the Amazon Basin, Geophysical Research Letters, 42, 5587–5593, doi:10.1002/2015GL064068, http://dx.doi.org/10.1002/2015GL064068, 2015GL064068, 2015.

Stephens, G. L., Vane, D. G., Boain, R. J., Mace, G. G., Sassen, K., Wang, Z., Illingworth, A. J., O'Connor, E. J., Rossow, W. B., Durden, S. L., Miller, S. D., Austin, R. T., Benedetti, A., Mitrescu, C., and CloudSat Science Team, T.: THE CLOUDSAT MISSION AND THE A-TRAIN, Bull. Amer. Meteor. Soc., 83, 1771–1790, http://dx.doi.org/10.1175/BAMS-83-12-1771, 2002.

Sun, Z. and Shine, K. P.: Studies of the radiative properties of ice and mixed-phase clouds, Quarterly Journal of the Royal Meteorological Society, 120, 111–137, doi:10.1002/qj.49712051508, 1994.

Tao, W.-K. and Moncrieff, M. W.: Multiscale cloud system modeling, Reviews of Geophysics, 47, RG4002, doi:10.1029/2008RG000276, 2009.

Wandinger, U.: Observation of Aerosol-Cloud-Turbulence Interaction with Integrated Remote-Sensing Instrumentation, in: Proceedings 26th ILRC, 2012.

Yano, J.-I. and Phillips, V. T. J.: Ice–Ice Collisions: An Ice Multiplication Process in Atmospheric Clouds, J. Atmos. Sci., 68, 322–333, http://dx.doi.org/10.1175/2010JAS3607.1, 2010.